PLOS | ONE

RESEARCH ARTICLE

Fluorogenic Substrates for *In Situ* Monitoring of Caspase-3 Activity in Live Cells

Ana M. Pérez-López[1], M. Lourdes Soria-Gila[2], Emma R. Marsden[1], Annamaria Lilienkampf[1], Mark Bradley[1]*

1 School of Chemistry, EaStCHEM, University of Edinburgh, Joseph Black building, West Mains Road, Edinburgh EH9 3FJ, United Kingdom, **2** Department of Medicinal and Organic Chemistry, University of Granada, School of Pharmacy, Campus Cartuja s/n – 18071, Granada, Spain

* mark.bradley@ed.ac.uk

Citation: Pérez-López AM, Soria-Gila ML, Marsden ER, Lilienkampf A, Bradley M (2016) Fluorogenic Substrates for *In Situ* Monitoring of Caspase-3 Activity in Live Cells. PLoS ONE 11(5): e0153209. doi:10.1371/journal.pone.0153209

Editor: Shawn B Bratton, The University of Texas MD Anderson Cancer Center, UNITED STATES

Received: November 17, 2015

Accepted: March 26, 2016

Published: May 11, 2016

Data Availability Statement: All relevant data are within the paper and its Supporting Information files.

Funding: This work was supported by the Ramon Areces and Caja Madrid Foundations to AMPL and Spanish Ministry of Economy and Competitiveness to MLSG (graduate student fellowships FPI BES-2010-030257 and EEBB-I-13-07131). The funders had no role in study design, data collection and analysis, decision to publish, or preparation of the manuscript.

Competing Interests: The authors have declared that no competing interests exist.

Abstract

The *in situ* detection of caspase-3 activity has applications in the imaging and monitoring of multiple pathologies, notably cancer. A series of cell penetrating FRET-based fluorogenic substrates were designed and synthesised for the detection of caspase-3 in live cells. A variety of modifications of the classical caspase-3 and caspase-7 substrate sequence Asp-Glu-Val-Asp were carried out in order to increase caspase-3 affinity and eliminate caspase-7 cross-reactivity. To allow cellular uptake and good solubility, the substrates were conjugated to a cationic peptoid. The most selective fluorogenic substrate **27**, FAM-Ahx-Asp-Leu-Pro-Asp-Lys(MR)-Ahx, conjugated to the cell penetrating peptoid at the C-terminus, was able to detect and quantify caspase-3 activity in apoptotic cells without cross-reactivity by caspase-7.

Introduction

Fluorogenic substrates and activity-based probes enable the study of protease function and have been used to elucidate the role of caspases in the progression of diseases such as cancer [1–6], neurodegenerative disorders [7–10], and sepsis [11,12]. Caspases are an important family of cysteine-dependent aspartate proteases that exist within cells as inactive zymogens with their cleavage giving active enzymes initiating cellular apoptosis [13–15]. Inappropriate control of this apoptotic machinery is implicated in many diseases [14,15], notably cancer [16,17]. As a part of the apoptotic cascade, executioner caspase-3 activates several important cellular substrates [14–20], such as PARP and ICAD, and its decreased activity is a prognostic indicator of chemoresistance in breast and ovarian cancer [21,22]. The ability to monitor caspase-3 activity *in situ* could provide a means, not only to elucidate its complex role in biological processes, but also to monitor the efficacy of anticancer drugs and to identify patients for whom discontinuation of ineffective toxic treatment is warranted, for example, due to acquired drug resistance [23].

Current methods are able to detect caspase-3 activity *in vitro* although they often display promiscuity and cannot be used to monitor caspase-3 within cells [24–26]. The majority of

fluorogenic caspase-3 substrates are based on a four-residue recognition sequence Asp-Glu-Val-Asp (DEVD) [23,27,28], established via combinatorial library methods [29,30]; however, this sequence is also efficiently cleaved by caspase-7, which shares very similar substrate specificities with caspase-3. In mouse macrophages, 46 out of the 55 identified protein cleavage sites (within 48 proteins) were cleaved by both enzymes with only 3 sites specifically cleaved by caspase-3 [31]. Incorporation of unnatural amino acids into the recognition sequence has yielded caspase-3 substrates with increased selectivity [32,33]. Recently, Wolan achieved live cell imaging of caspase-3 activity in apoptotic cells, with selectivity over caspase-7, with a near-infrared fluorogenic pentapeptide substrate (incorporating the unnatural amino acid β-homo-Leu) coupled to a cell penetrating peptide derived from the viral SV40 Large T-antigen nuclear localising signal [34].

Here, FRET-based fluorogenic substrates, incorporating a tetrapeptide recognition sequence Asp-X_3-X_2-Asp, were designed and synthesised for the selective, *in situ* monitoring of caspase-3 activity. To allow detection in live cells, the substrates were conjugated to a cationic peptoid-based cellular delivery vehicle.

Results and Discussion

Substrate design and synthesis

In order to improve selectivity towards caspase-3 over caspase-7, permutations of the classical tetrapeptide substrate Asp-Glu-Val-Asp (X_4-X_3-X_2-X_1) were explored. All known caspase-3 substrates contain Asp at position X_1 and 80% contain an Asp at the X_4 position of the sequence. The positions X_3 and X_2 are more varied, with no clear amino acid preference being reported for the X_3 position (~20% of the substrates contain Glu and ~15% Phe or Val at this position). Approximately 40% of known caspase-3 substrates contain Val at the X_2 position; however, Pro at the X_2 position is known to increase specificity for caspase-3 over caspase-7 [35]. With the aim of improving caspase-3 selectivity, X_3 and X_2 modifications of the tetrapeptide sequence were carried out, retaining Asp at X_1 and X_4 positions. The X_3 position was changed to Pro, Gly, Ala, Leu, Asn and Val, and the X_2 position had Val (substrates **1**–**9**) or Pro (substrates **10**–**14**) (Table 1) [36,37]. For each substrate, the corresponding d-amino acid sequence was synthesised as a control (compounds **15**–**24**, respectively, see ESI). 5(6)-Carboxyfluorescein was coupled to the N-terminus of the substrates via a 6-aminohexanoic acid (Ahx) spacer, and a quencher moiety was introduced next to the caspase cleavage site via Lys side chain modification (separated by an Ahx spacer from the Asp-X_3-X_2-Asp) (Fig 1). As the choice of the quencher can affect the rate of cleavage and level of background fluorescence, three different quenchers, methyl red (MR), Black Hole Quencher®-1 (BHQ1), and 5(6)-carboxytetraethylrhodamine (TAMRA) were evaluated. A cationic, "lysine-like" nonaresidue peptoid was incorporated onto the C-terminus to ensure cellular uptake of the substrates [38]. Unlike many common cell penetrating peptides [39–41] this peptoid is resistant to proteolysis, non-toxic *in vivo*, and has demonstrated a highly efficient cell entry profile [42–44]. In addition, peptoid-based delivery systems are not prone producing immunogenic responses associated with virus-derived sequences [45,46].

The peptides **1**–**14** and controls **15**–**24** were synthesised on a Rink amide-functionalised aminomethyl polystyrene resin (1% DVB, 100–200 mesh, loading 1.2 mmol/g) using an Fmoc/^{t}Bu-based strategy with microwave heating (S1 Fig) [47]. First, the nonapeptoid was synthesised using *N*-Fmoc-(6-Boc-aminohexyl)glycine [48] and DIC and Oxyma. Fmoc-Lys (Dde)-OH was coupled onto the peptoid, followed by Fmoc-Ahx-OH, and the substrate sequence (Asp-X_2-X_1-Asp), Fmoc-Ahx-OH, and 5(6)-carboxyfluorescein. The Lys side chain Dde protecting group was selectively removed with 2% hydrazine (v/v), followed by coupling

Table 1. The recognition sequence is a tetrapeptide (X_4-X_3-X_2-X_1) with two variable positions. X_1 and X_4 was Asp in all peptides. Three different quenchers, methyl red (MR), Black Hole Quencher®-1 (BHQ1), and 5(6)-carboxytetraethylrhodamine (TAMRA) were evaluated. As controls, substrates were also synthesised with the corresponding d-amino acid sequence (compounds **15**–**24**, respectively, see supporting information). For full structures, see Fig 1.

substrate	X_4-X_3-X_2-X_1	quencher (Q)
1	Asp-Glu-Val-Asp	MR
2	Asp-Glu-Val-Asp	TAMRA
3	Asp-Glu-Val-Asp	BHQ1
4	Asp-Pro-Val-Asp	MR
5	Asp-Gly-Val-Asp	MR
6	Asp-Ala-Val-Asp	MR
7	Asp-Leu-Val-Asp	MR
8	Asp-Asn-Val-Asp	MR
9	Asp-Val-Val-Asp	MR
10	Asp-Gly-Pro-Asp	MR
11	Asp-Ala-Pro-Asp	MR
12	Asp-Leu-Pro-Asp	MR
13	Asp-Asn-Pro-Asp	MR
14	Asp-Val-Pro-Asp	MR

doi:10.1371/journal.pone.0153209.t001

of the carboxy-functionalised quencher. After deprotection and cleavage from the resin with TFA–TIS–DCM, peptides **1**–**24** were purified by preparative HPLC and analysed by MALDI--TOF MS.

The effect of the quencher on caspase-3 cleavage

To optimise the fluorogenic substrates, MR (λ_{Abs} 480 nm), TAMRA (λ_{Abs} 555 nm), and BHQ1 (λ_{Abs} 534 nm) were evaluated as quenchers for 5(6)-carboxyfluorescein ($\lambda_{Ex/Em}$ 488/528 nm) in compounds **1**, **2** and **3**, using the classical substrate Asp-Glu-Val-Asp. Only **1** (MR as quencher) showed notable time-dependent increase in fluorescence upon incubation with caspase-3 and 7 (**2** and **3**, incorporating TAMRA and BHQ1, did not demonstrate significant increase in fluorescence) (Fig 2).

Kinetic studies with Caspase-3 and 7

The ability of **1** and **5**–**24** (bearing MR as the quencher of choice) to act as s substrate for caspase-3, as well as caspase-7, was investigated by determining the catalytic efficiency (k_{cat}/K_M) for each substrate with both enzymes (Table 2). None of the d-amino acids containing sequences **15**–**24** or **4**, which has a Pro residue at position X_3, showed any change in fluorescence intensity over time. With caspase-3, all the substrates with Val in X_2 position (substrates **5**–**9**) showed similar catalytic efficiency (k_{cat}/K_M 0.7–2.0 $\mu M^{-1}min^{-1}$) as Asp-Glu-Val-Asp (substrate **1**, 1.4 $\mu M^{-1}min^{-1}$). Substrate **5** (Asp-Gly-Val-Asp) showed 5-fold selectivity over caspase-7 (Table 2). Pro at the X_2 position increased specificity for caspase-3 over caspase-7 [49], particularly with substrates **11** (Asp-Ala-Pro-Asp), **12** (Asp-Leu-Pro-Asp) and **14** (Asp-Val-Pro-Asp), which exhibited 8–20-fold selectivity over caspase-7, along with increased caspase-3 affinity (K_M 0.2–0.4 μM) and catalytic effiency (k_{cat}/K_M 3.4–8.1 $\mu M^{-1}min^{-1}$).

To confirm how specific **11**, **12** and **14** were for caspase-3, these substrates were incubated with high enzyme concentrations (10–20 μM substrate, 0.4 μM enzyme) and the caspase-mediated cleavage analysed by MALDI-TOF MS. As expected, all the substrates were cleaved by

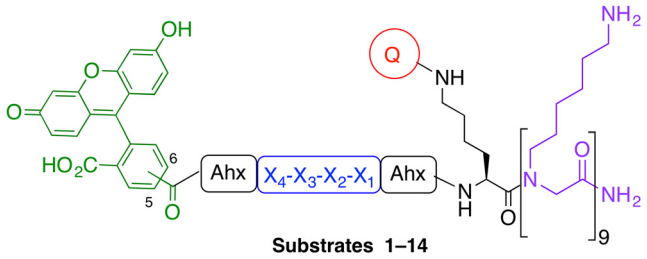

Fig 1. The design of the FRET-based fluorogenic tetrapeptide substrates for caspase-3 detection in live cells. The substrates bear 5(6)-carboxyfluorescein ($\lambda_{Ex/Em}$ 488/528 nm) at the amino-terminus and a quencher coupled via a Lys side-chain. The recognition sequence is a tetrapeptide (Asp-X_3-X_2-Asp) with two variable positions (see Table 1). The C-terminus bears a "lysine-like" nonaresidue peptoid to enable cellular uptake.

doi:10.1371/journal.pone.0153209.g001

caspase-3 at the X_1 position (between Asp and the Ahx spacer), with the parent compound no longer detected after 2h; however, these substrates were also (partially) cleaved by caspase-7. Remarkably, MS analysis revealed that that caspase-7 exhibited a different cleavage pattern cleaving the substrates between the Ahx spacer and the Lys(MR) (S2–S4 Figs).

Substrate optimisation

To eliminate the caspase-7 cross reactivity, three new substrates, all bearing Asp-Leu-Pro-Asp, were synthesised using d-Lys or *N*-Methyl-Lys as the quencher attachment point (**25** and **26**, respectively) and switching the position of the Ahx spacer (**27**) (Fig 3). Substrate **25** was cleaved by both caspase-3 and 7, whereas the *N*-methylated substrate **26** was not cleavage by either enzyme (S6 and S7 Figs). Substrate **27** showed good affinity for caspase-3 (K_M 1.1 ± 0.3 μM) with k_{cat} of 2.1 ± 0.8 min^{-1} and a catalytic efficiency of 0.5 ± 0.08 $\mu M^{-1}min^{-1}$. Remarkably, caspase-7 (0.4 μM) did not show any cleavage of this substrate (S7 and S8 Figs).

Detecting caspase-3 activity in live cells

Caspase-3 activity in HEK293T cells was evaluated using the caspase-3 selective substrate **27** with apoptosis induced by staurosporine. Flow cytometry analysis of cells treated with **27**

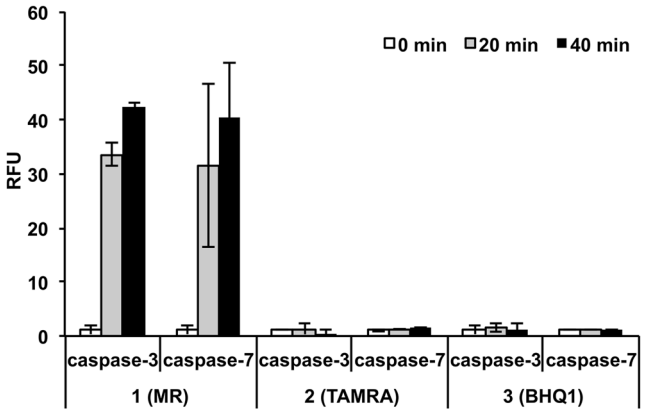

Fig 2. Relative increase in fluorescence intensity of the FRET-based peptides, bearing different quenchers (MR, TAMRA or BHQ1) on the Lys side chain, after incubation with caspase-3 and 7. The FRET-based peptides **1**, **2** and **3** (6 μM) were incubated with caspase-3 and 7 (20 nM) and fluorescence recorded at 10, 20 and 40 min (n = 3, normalised to zero).

doi:10.1371/journal.pone.0153209.g002

Table 2. Kinetic analysis of the fluorogenic substrates. The kinetic parameters (n = 3) were determined for the fluorogenic substrates **1** and **5**–**14** (measured using substrate range of 0.1–8 μM) with caspase-3 and caspase-7. Substrate **4** or the d-amino acids containing **15**–**24** were not cleaved by either enzyme.

	Caspase-3			Caspase-7		
	K_M (μM)	*Kcat* (min^{-1})	*kcat*/ K_M ($\mu M^{-1}min^{-1}$)	K_M (μM)	*kcat* (min^{-1})	*kcat*/ K_M ($\mu M^{-1}min^{-1}$)
1	0.6 ± 0.1	0.9 ± 0.04	1.4	0.5 ± 0.1	1.1 ± 0.1	2.1
5	0.3 ± 0.1	0.5 ± 0.03	1.7	1.2 ± 0.2	0.4 ± 0.1	0.3
6	1.5 ± 0.4	1.1 ± 0.1	0.7	14.0 ± 3.4	19.2 ± 1.6	1.4
7	0.8 ± 0.2	0.9 ± 0.1	1.2	0.9 ± 0.2	1.0 ± 0.1	1.1
8	0.4 ± 0.1	0.8 ± 0.04	2.0	0.6 ± 0.1	0.8 ± 0.03	1.3
9	1.8 ± 0.4	1.4 ± 0.1	0.8	4.1 ± 0.6	1.8 ± 0.1	0.4
10	0.7 ± 0.4	0.55 ± 0.2	0.8	0.3 ± 0.05	0.2 ± 0.01	0.6
11	0.4 ± 0.1	1.3 ± 0.1	3.4	4.9 ± 2.1	1.6 ± 0.3	0.3
12	0.2 ± 0.1	1.4 ± 0.2	5.8	1.4 ± 0.3	0.9 ± 0.07	0.7
13	0.8 ± 0.2	1.0 ± 0.2	1.2	1.2 ± 0.2	1.0 ± 0.06	0.8
14	0.2 ± 0.04	1.7 ± 0.1	8.1	3.6 ± 0.9	1.4 ± 0.2	0.4

doi:10.1371/journal.pone.0153209.t002

(10 μM) showed a 2.5-fold increase in the fluorescence intensity ($\lambda_{Ex/Em}$ 488/530 nm) of the cells after apoptotic stimulation by staurosporine (1 μM), with no increase observed in fluoresce without it (Fig 4). This increase in fluorescence with substrate **27** suggested that the concentration of caspase-3 in apoptotic cells was approximately 15.7 ± 0.5 nM per cell (28271 molecules per cell) in the execution phase of apoptosis (based on the *Vmax* and the *kcat* of **27**, see supporting information) [50]. In live-cell confocal imaging of caspase-3 activation with **27** (10 μM), fluorescence "turn-on" was only detected in the cytoplasm of apoptotic HEK293T cells, with no increase in fluorescence observed in non-apoptotic cells (Fig 5A, 5B and S9 Fig). No fluorescence "turn-on" was observed in apoptotic MCF-7 cells (Fig 5C), which lack functional caspase-3 but express caspase-7 [34,51,52], confirming the isoform selectivity. Substrate **27** was nontoxic in an MTT assay at 10 μM concentration (S10 Fig).

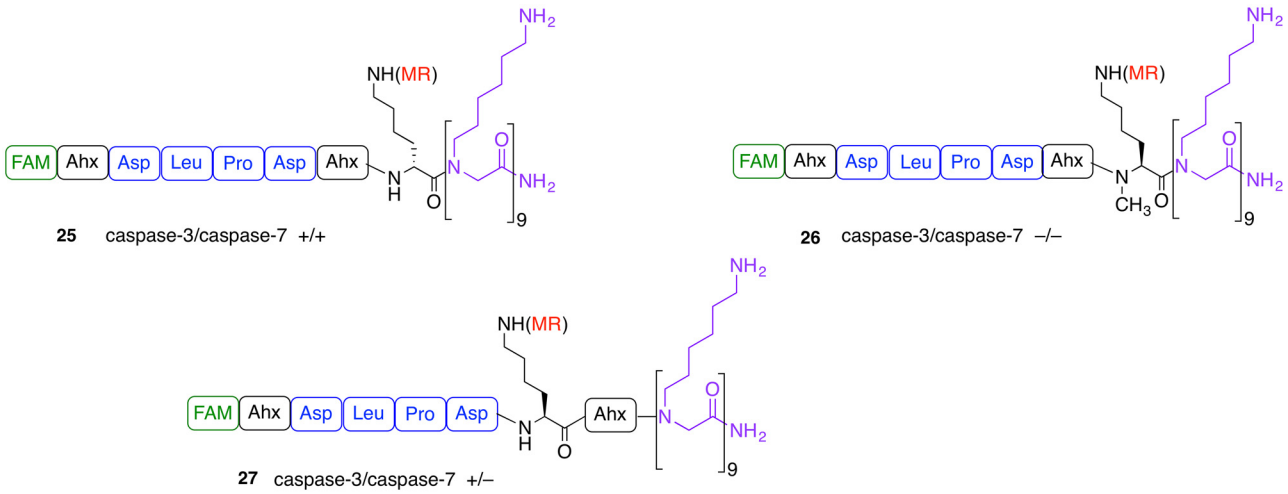

Fig 3. Structural modifications to the fluorogenic substrates with the aim of eliminating caspase-7 cross-reactivity. Substrate **25** has a D-Lys residue, **26** an *N*-Methyl-Lys, and in substrate **27** the Ahx spacer has been moved between the Lys and the peptoid moiety. Caspase-3 selectivity was achieved with **27**.

doi:10.1371/journal.pone.0153209.g003

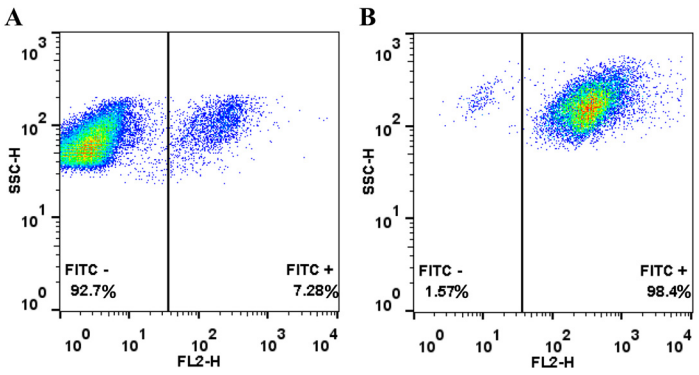

Fig 4. Flow cytometry analysis of healthy and apoptotic HEK293T cells treated with substrate 27. The cells were incubated 5 h with fluorogenic substrate **27** (10 μM), detached, and analysed by flow cytometry ($\lambda_{Ex/Em}$ 488/530 nm, x-axis = fluorescence intensity). (A) Healthy, non-apoptotic cells. (B) Apoptotic cells (induced by 1 μM staurosporine).

doi:10.1371/journal.pone.0153209.g004

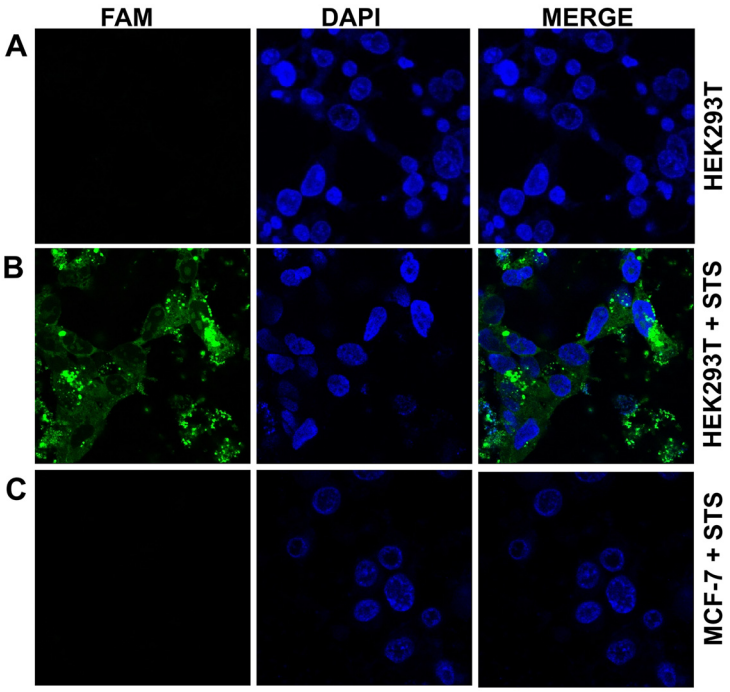

Fig 5. Confocal microscopy images of HEK293T and MCF-7 cells treated with substrate 27. Confocal microscopy images (objective HCX PL APO ×63/1.40–0.6 Oil CS) of HEK273T cells with substrate **27** (10 μM) without staurosporine (STS) (**A**) and with staurosporine (1 μM) (**B**) induced apoptosis (green fluorescence is from fluorescein "turned on" by caspase-3 cleavage of the substrate, blue is DAPI nuclear stain). (**C**) Staurosporine treated MCF-7 cells with substrate **27**.

doi:10.1371/journal.pone.0153209.g005

Conclusions

Fluorogenic, FRET-based substrates for monitoring the enzymatic activity of caspase-3 *in situ* were synthesised with permutations of the substrate sequence Asp-X_2-X_3-Asp with the aim of improving selectivity for caspase-3 over caspase-7. The fluorogenic substrates had 5(6)-carboxyfluorescein in the amino-terminus and an optimised quencher, methyl red, introduced via Lys

side chain modification. These fluorogenic substrates were conjugated at the C-terminus to a cationic cell delivery vehicle to allow efficient cellular uptake. Substrates with Pro in the X_2 position (instead of Val), showed selectivity for caspase-3 over caspase-7, along with increased caspase-3 affinity, particularly when X_3 was Ala, Leu or Val. Mass spectrometry studies revealed unexpected cleavage pattern of the fluorogenic substrates with caspase-7, while optimisation of the substrate via spacer relocation yielded a caspase-3 selective substrate **27** (FAM-Ahx-Asp-Leu-Pro-Asp-Lys(MR)-Ahx-peptoid). In apoptotic cells, the optimised substrate **27** allowed imaging of caspase-3 activity *in situ*. Flow cytometry analysis gave approximate quantification of the concentration of caspase-3 in a cell to be 16 nM (28271 molecules per cell). Future work is aimed at the use of this caspase-3 selective sequence in *in vivo* near-infrared fluorescence imaging techniques, especially for cancer, which require stable, highly specific, and sensitive fluorogenic substrates.

Materials and Methods

Synthesis of fluorogenic substrates 1–27

A highly optimised microwave-based solid–phase strategy was used to synthesise the cell penetrating peptide–peptoids [38]. All solvents and reagents were obtained from commercial suppliers and used without purification. A Rink-amide functionalised aminomethyl polystyrene (1% DVB, 100–200 mesh, loading 1.2 mmol/g) resin was used for the synthesis of the peptides with an Fmoc-based strategy (S1 Fig). **Coupling of the Fmoc-amino acids and fluorophores:** The resin (1 eq) was pre-swollen in DCM, washed with DMF, and added a pre-activated mixture (10 min) of the carboxylic acid (3 eq), DIC (3 eq) and Oxyma (3 eq) in DMF (0.1 M). This reaction mixture was stirred in the microwave (Biotage Initiator) for 20 minutes at 60°C after which the resin was washed with DMF, DCM and MeOH. **Fmoc deprotection:** The resin was shaken with 20% piperidine in DMF (2 ×10 min), and subsequently washed with DMF, DCM and MeOH. **Dde deprotection:** The resin was shaken with 2% hydrazine in DMF (v/v) (2 ×10 min), and subsequently washed with DMF, DCM and MeOH. **Cleavage from the resin and deprotection:** A solution of TFA/TIS/DCM (90:5:5) was added to the resin (20 μL of the cleavage cocktail per mg of resin) and left to shake for 5 hours. The resin was filtrated and washed with DCM, and the collected filtrate was evaporated under reduced pressure and the compound precipitated using cold diethyl ether. Peptides **1**–**24** were purified by preparative HPLC and analysed by MALDI-TOF MS. For the characterisation of the peptides, see S1 Table.

Kinetic assays with caspase-3 and 7

Caspase-3 or caspase-7 (R&D systems, USA) was added to 100 μL of caspase assay buffer with substrates **1**–**14** at concentrations from 0.1 μM to 8 μM in a 96-well plate (n = 3) to give final enzyme concentration of 20 nM (**1**–**9**) or 15 nM (**10**–**14**). Fluorescence ($\lambda_{Ex/Em}$ 485/528 nm) was recorded on a Biotek Synergy HT Multi-Mode Microplate Reader every 2 min. Control samples had the same composition but no enzyme. The rate (μM/min) was calibrated using a 5(6)-carboxyfluorescein conversion factor (0.0055 μM/RFU) and data plotted against time (min). For initial cleavage rate (0–5 min), plots were fitted using linear regression analysis and the Michaelis-Menten data generated using GraphPad Prism 5.

Caspase-3 detection in live cells

Cell culture was performed in a Heracell 150 incubator (Heraeus) and in a Herasafe KS 18 class II negative-flow cabinet (Heraeus). HEK293T and MCF-7 cells (cultured in high glucose (4.5 mg/mL) DMEM supplemented with 4 mM glutamine, 100 units/mL penicillin, 10 mg/mL

streptomycin and 25 mg/mL amphotericin B, and 10% FBS) were seeded onto a 48-well plate at a density of 10^4 cells per well. After 12 hours, the media was removed and substrates **1**–**14** added at 10 μM in fresh media. Selected wells were also treated with staurosporine (1 μM). After 5 hours, the cells were washed twice with PBS, detached with trypsin/EDTA, harvested with 2% FBS in PBS supplemented with Trypan Blue (0.04%) for analysis on a BD FACSAria® flow cytometer. Fluorescence was evaluated as mean fluorescence intensity (MFI) and estimated <100 u.a. for untreated control cells (consistent values independently of staurosporine addition). Apoptotic cells treated with substrate **1** were used as a positive control to obtain the maximum of fluorescence signal. 50,000 events per sample were plotted in two-dimensional dot plots based on forward and side scattering. The cellular size and complexity (SSC-H vs. FSC-H) were used to gate two populations (alive/apoptotic cells) (debri excluded). The data were analysed using the software Flowjo® 7.5.

For confocal microscopy, the cells were fixed with 4% paraformaldehyde in PBS and the nuclei stained with Hoechst-33342 (1% w/v in PBS). Cellular fluorescence of cells was analysed using an Inverted Leica DM IRB with filter I3 (450–490 nm) and a Leica SP5 Confocal (FITC and DAPI channel).

Supporting Information

S1 Fig. Solid phase synthesis of the fluorogenic substrates 1–24.
(PDF)

S2 Fig. MALDI-TOF MS spectra of substrate 11.
(PDF)

S3 Fig. MALDI-TOF MS spectra of substrate 12.
(PDF)

S4 Fig. MALDI-TOF MS spectra of substrate 14.
(PDF)

S5 Fig. MALDI-TOF MS spectra of substrate 25.
(PDF)

S6 Fig. MALDI-TOF MS spectra of 26.
(PDF)

S7 Fig. Analysis of substrate 27 with caspase-3 and caspase-7.
(PDF)

S8 Fig. MALDI-TOF MS spectra of 27.
(PDF)

S9 Fig. Substrate 27 selectively labels apoptotic cells.
(PDF)

S10 Fig. Cell viability.
(PDF)

S1 File. Quantification of caspase-3 in apoptotic cells by flow cytometry.
(PDF)

S1 Table. MALDI-TOF MS and HPLC analysis of substrates 1–27.
(PDF)

Author Contributions

Conceived and designed the experiments: AMPL MLSG AL MB. Performed the experiments: AMPL MLSG ERM. Analyzed the data: AMPL MLSG AL MB. Wrote the paper: AL AMPL MB.

References

1. Tsai FY, Greenbaum DC, Hager JH, Bogyo M, Hanahan D. Cathepsin cysteine proteases are effectors of invasive growth and angiogenesis during multistage tumorigenesis. Cancer Cell 2004; 5: 443–453. PMID: 15144952
2. Speers AE, Cravatt BF. Profiling enzyme activities in vivo using click chemistry methods. Chem Biol. 2004; 11: 535–546. PMID: 15123248
3. Paulick MG, Bogyo M. Application of activity-based probes to the study of enzymes involved in cancer progression. Curr Opin Genet Dev. 2008; 18: 97–106. doi: 10.1016/j.gde.2007.12.001 PMID: 18294838
4. Edgington LE, Berger AB, Blum G, Albrow VE, Paulick MG, Lineberry N, et al. Noninvasive optical imaging of apoptosis by caspase-targeted activity-based probes. Nat Med. 2009; 15: 967–973. doi: 10.1038/nm.1938 PMID: 19597506
5. Nomura DK, Dix MM, Cravatt BF. Activity-based protein profiling for biochemical pathway discovery in cancer. Nat Rev Cancer. 2010; 10: 630–638. doi: 10.1038/nrc2901 PMID: 20703252
6. Edgington LE, Verdoes M, Ortega A, Withana NP, Lee J, Syed S, et al. Functional imaging of legumain in cancer using a new quenched activity-based probe. J Am Chem Soc. 2013; 135: 174–182. doi: 10.1021/ja307083b PMID: 23215039
7. Graham RK, Deng Y, Slow E, Haigh B, Bissada N, Lu G, et al. Cleavage at the caspase-6 site is required for neuronal dysfunction and degeneration due to mutant huntingtin. Cell. 2006; 125: 1179–1191. PMID: 16777606
8. Leyva MJ, Degiacomo F, Kaltenbach LS, Holcomb J, Zhang N, Gafni J, et al. Identification and evaluation of small molecule pan-caspase inhibitors in Huntington's disease models. Chem Biol. 2010; 17: 1189–1200. doi: 10.1016/j.chembiol.2010.08.014 PMID: 21095569
9. Edgington LE, van Raam BJ, Verdoes M, Wierschem C, Salvesen GS, Bogyo M. An optimized activity-based probe for the study of caspase-6 activation. Chem Biol. 2012; 19: 340–352. doi: 10.1016/j.chembiol.2011.12.021 PMID: 22444589
10. D'Amelio M, Sheng M, Cecconi F. Caspase-3 in the central nervous system: beyond apoptosis. Trends Neurosci. 2012; 35: 700–709. doi: 10.1016/j.tins.2012.06.004 PMID: 22796265
11. Hotchkiss RS, Chang KC, Swanson PE, Tinsley KW, Hui JJ, Klender P, et al. Caspase inhibitors improve survival in sepsis: a critical role of the lymphocyte. Nat Immunol. 2000; 1: 496–501. PMID: 11101871
12. Hotchkiss RS, Nicholson DW. Apoptosis and caspases regulate death and inflammation in sepsis. Nat Rev Immunol. 2006; 6: 813–822. PMID: 17039247
13. Van Damme P, Martens L, Van Damme J, Hugelier K, Staes A, Vandekerckhove J, et al. Caspase-specific and nonspecific in vivo protein processing during Fas-induced apoptosis. Nat Methods. 2005; 2: 771–777. PMID: 16179924
14. Tanuma S, In Apoptosis in Normal Development and Cancer; Sluyser M., Ed.; Taylor and Francis: London, 1996; pp 39–59.
15. Thompson CB, Apoptosis in the pathogenesis and treatment of disease. Science. 1995; 267: 1456–1462. PMID: 7878464
16. Nicholson DW. From bench to clinic with apoptosis-based therapeutic agents. Nature. 2000; 407: 810–816. PMID: 11048733
17. Wyllie AH, Bellamy CO, Bubb VJ, Clarke AR, Corbet S, Curtis L. Apoptosis and carcinogenesis. Br J Cancer. 1999; 80: 34–37. PMID: 10466759
18. Potten CS, Booth C. The role of radiation-induced and spontaneous apoptosis in the homeostasis of the gastrointestinal epithelium: a brief review. Comp Biochem Physiol. 1997; 118: 473–478.
19. Green DR, Apoptotic pathways: paper wraps stone blunts scissors. Cell. 2000; 102: 1–4. PMID: 10929706
20. Enari M, Sakahira H, Yokoyama H, Okawa K, Iwamatsu A, Nagata S. A caspase-activated DNase that degrades DNA during apoptosis, and its inhibitor ICAD. Nature. 1998; 391: 43–50. PMID: 9422506

21. Devarajan E, Sahin AA, Chen JS, Krishnamurthy RR, Aggarwal N, Brun AM, et al. Down-regulation of caspase 3 in breast cancer: a possible mechanism for chemoresistance. Oncogene. 2002; 21: 8843–8851. PMID: 12483536

22. Ai H, Hazelwood KL, Davidson MW, Campbell RE. Fluorescent protein FRET pairs for ratiometric imaging of dual biosensors. Nat Methods. 2008; 5: 401–403. doi: 10.1038/nmeth.1207 PMID: 18425137

23. Savitsky AP, Rusanov AL, Zherdeva V, Gorodnicheva T, Khrenova MG, Nemukhin AV. FLIM-FRET Imaging of Caspase-3 activity in live cells using pair of red fluorescent proteins. Theranostics. 2012; 2: 215–226. doi: 10.7150/thno.3885 PMID: 22375160

24. Kuida K, Zheng TS, Na S, Kuan C, Yang D, Karasuyama H, et al. Decreased apoptosis in the brain and premature lethality in CPP32-deficient mice. Nature. 1996; 384: 368–372. PMID: 8934524

25. Agniswamy J, Fang B, Weber IT. Plasticity of S2-S4 specificity pockets of executioner caspase-7 revealed by structural and kinetic analysis. FEBS J. 2007; 274: 4752–4765. PMID: 17697120

26. McStay GP, Salvesen GS, Green DR. Overlapping cleavage motif selectivity of caspases: implications for analysis of apoptotic pathways. Cell Death Differ. 2008; 15: 322–331. PMID: 17975551

27. Cardenas-Maestre JM, Perez-Lopez AM, Bradley M, Sanchez-Martin RM. Microsphere-based intracellular sensing of caspase-3/7 in apoptotic living cells. Macromol Biosci. 2014; 14: 923–928. doi: 10.1002/mabi.201300525 PMID: 24664851

28. Laxman B, Hall DE, Bhojani MS, Hamstra DA, Chenevert TL, Ross BD, et al. Noninvasive real-time imaging of apoptosis. Proc Natl Acad Sci USA. 2002; 99: 16551–16555. PMID: 12475931

29. Germain M, Affar EB, D'Amours D, Dixit VM, Salvesen GS, Poirier GG. Cleavage of automodified poly (ADP-ribose) polymerase during apoptosis. Evidence for involvement of caspase-7. J Biol Chem. 1999; 274: 28379–28384. PMID: 10497198

30. Thornberry NA, Rano TA, Peterson EP, Rasper DM, Timkey T, Garcia-Calvo M, et al. A combinatorial approach defines specificities of members of the caspase family and granzyme B. Functional relationships established for key mediators of apoptosis. J Biol Chem. 1997; 272: 17907–17911. PMID: 9218414

31. Demon D, Van Damme P, Vanden Berghe T, Deceuninck A, Van Durme J, Verspurten J, et al. Proteome-wide substrate analysis indicates substrate exclusion as a mechanism to generate caspase-7 versus caspase-3 specificity. Mol Cell Proteomics. 2009; 12: 2700–2714.

32. Poreba M, Kasperkiewicz P, Snipas SJ, Fasci D, Salvesen GS, Drag M. Unnatural amino acids increase sensitivity and provide for the design of highly selective caspase substrates. Cell Death Differ. 2014; 21: 1482–1492. doi: 10.1038/cdd.2014.64 PMID: 24832467

33. Vickers CJ, Gonzaález-Paáez GE, Wolan DW. Selective detection of caspase-3 versus caspase-7 using activity-based probes with key unnatural amino acids. ACS Chem Biol. 2013; 8: 1558–1566. doi: 10.1021/cb400209w PMID: 23614665

34. Vickers CJ, Gonzalez-Paez GE, Wolan DW. Discovery of a highly selective caspase-3 substrate for imaging live cells. ACS Chem Biol. 2014; 9: 2199–2203. doi: 10.1021/cb500586p PMID: 25133295

35. Lien S, Pastor R, Sutherlin D, Lowman HB. A substrate-phage approach for investigating caspase specificity. Protein J. 2004; 23: 413–425. PMID: 15517988

36. Wu H, Ge J, Yang P, Wang J, Uttamchandani M, Yao S. A peptide aldehyde microarray for high-throughput profiling of cellular events. J Am Chem Soc. 2011; 133: 1946–1954. doi: 10.1021/ja109597v PMID: 21247160

37. Boulware K, Daugherty P. Protease specificity determination by using cellular libraries of peptide substrates (CLiPS). Proc Natl Acad Sci USA. 2006; 103: 7583–7588. PMID: 16672368

38. Unciti-Broceta A, Diezmann F, Ou-Yang CY, Fara MA, Bradley M. Synthesis, penetrability and intracellular targeting of fluorescein-tagged peptoids and peptide-peptoid hybrids. Bioorg Med Chem. 2009; 3: 959–966.

39. Vries E. TAT peptide internalization: seeking the mechanism of entry. Curr Protein Pept Sci. 2003; 4: 125–132. PMID: 12678851

40. Snyder EL, Dowdy SF. Cell penetrating peptides in drug delivery. Pharm Res. 2004; 21: 389–393. PMID: 15070086

41. Järver P, Langel U. The use of cell-penetrating peptides as a tool for gene regulation. Drug Discov Today. 2004; 9: 395–402. PMID: 15081956

42. Dhaliwal K, Alexander L, Escher G, Unciti-Broceta A, Jansen M, McDonald N, et al. M. Multi-modal molecular imaging approaches to detect primary cells in preclinical models. Faraday Discussions. 2011; 149: 107–114. PMID: 21413177

43. Kumar P, Fara MA, Bradley M, Healy E. Peptoid modification of alpha-melanocyte stimulating hormone to enhance penetration into skin. Br J Dermatol. 2006; 155: 237–237.

44. Healy E, Friedmann P, Bradley M. Topical Drug Delivery. WO 2007113531.

45. Langel U. Cell-penetrating peptides-Processes and applications. Pharmacology and Toxicology (Boca Raton, Fla), 2002, 245–262.

46. Lam AP, Dean DA. Progress and prospects: nuclear import of nonviral vectors. Gene Ther. 2010; 17: 439–447. doi: 10.1038/gt.2010.31 PMID: 20200566

47. Fara MA, Diaz-Mochon JJ, Bradley M. Microwave-assisted coupling with DIC/HOBt for the synthesis of difficult peptoids and fluorescently labelled peptides—a gentle heat goes a long way. Tetrahedron Lett. 2006; 47: 1011–1014.

48. Jong T, Pérez-López AM, Johansson EMV, Lilienkampf A, Bradley M. Flow and Microwave-Assisted Synthesis of N-(Triethylene glycol)glycine Oligomers and Their Remarkable Cellular Transporter Activities. Bioconj Chem. 2015; 26: 1759–1765.

49. Mackay M, Pérez-López AM. Bradley M, Lilienkampf A. Eliminating caspase-7 and cathepsin B cross-reactivity on fluorogenic caspase-3 substrates. Mol BioSyst. 2016; 12, 693–696. doi: 10.1039/c5mb00730e PMID: 26726961

50. Saunders PA, Cooper JA, Roodell MM, Schroeder DA, Borchert CJ, Isaacson AL, et al. Quantification of Active Caspase 3 in Apoptotic Cells. Anal Biochem. 2000; 284:114–124. PMID: 10933864

51. Jänicke RU, Sprengart ML, Wati MR, Porter AG. Caspase-3 is required for DNA fragmentation and morphological changes associated with apoptosis. J Biol Chem. 1998, 273:9357–9360. PMID: 9545256

52. Walsh JG, Cullen SP, Sheridan C, Lüthi AU, Gerner C, Martin SJ. Executioner caspase-3 and caspase-7 are functionally distinct proteases. PNAS. 2008; 105: 12815–12819. doi: 10.1073/pnas.0707715105 PMID: 18723680